Predicting Skull Loading: Applying Multibody Dynamics Analysis to a Macaque Skull

NEIL CURTIS,[1]* KORNELIUS KUPCZIK,[2] PAUL O'HIGGINS,[3] MEHRAN MOAZEN,[1] AND MICHAEL FAGAN[1]

[1]Centre for Medical Engineering and Technology, University of Hull, Hull, United Kingdom
[2]Department of Human Evolution, Max Planck Institute for Evolutionary Anthropology, Leipzig, Germany
[3]Hull-York Medical School, University of York, York, United Kingdom

ABSTRACT

Evaluating stress and strain fields in anatomical structures is a way to test hypotheses that relate specific features of facial and skeletal morphology to mechanical loading. Engineering techniques such as finite element analysis are now commonly used to calculate stress and strain fields, but if we are to fully accept these methods we must be confident that the applied loading regimens are reasonable. Multibody dynamics analysis (MDA) is a relatively new three dimensional computer modeling technique that can be used to apply varying muscle forces to predict joint and bite forces during static and dynamic motions. The method ensures that equilibrium of the structure is maintained at all times, even for complex statically indeterminate problems, eliminating nonphysiological constraint conditions often seen with other approaches. This study describes the novel use of MDA to investigate the influence of different muscle representations on a macaque skull model (*Macaca fascicularis*), where muscle groups were represented by either a single, multiple, or wrapped muscle fibers. The impact of varying muscle representation on stress fields was assessed through additional finite element simulations. The MDA models highlighted that muscle forces varied with gape and that forces within individual muscle groups also varied; for example, the anterior strands of the superficial masseter were loaded to a greater extent than the posterior strands. The direction of the muscle force was altered when temporalis muscle wrapping was modeled, and was coupled with compressive contact forces applied to the frontal, parietal and temporal bones of the cranium during biting. Anat Rec, 291:491–501, 2008. © 2008 Wiley-Liss, Inc.

Key words: multibody dynamics analysis; finite element analysis; Macaque; bite force; muscle force

Analysis of motion and the stress/strain fields of the masticatory apparatus are of interest for many reasons. We may wish to explain or predict masticatory function in extinct or extant animals, or understand how stresses that contribute to the development and evolution of skull form are created, or examine which structures are related to stress alleviation and which are associated with display or protection of sensory organs. Bone is a dynamic structure that can modify its geometry in response to applied loads, and even though our understanding has increased in recent years (e.g., Huiskes,

Grant sponsor: the Leverhulme Trust; Grant sponsor: The Biotechnology and Biological Sciences Research Council (BBSRC).

*Correspondence to: Neil Curtis, Department of Engineering and Centre for Medical Engineering and Technology (CMET), University of Hull, Hull, HU67RX UK. Fax: 44(0)1482 466664. E-mail: n.curtis@hull.ac.uk

Received 11 December 2007; Accepted 30 January 2008

DOI 10.1002/ar.20689

Published online 31 March 2008 in Wiley InterScience (www.interscience.wiley.com).

2000; see, e.g., reviews in Pearson and Lieberman, 2004; Ruff et al., 2006), we have known about the relationship between bone loading and the development of bone morphology since the late 1800s (i.e., Wolff's Law; Wolff, 1892). In the facial skeletons of diverse New and Old World monkeys growth remodeling fields show considerable and, as yet unexplained, ontogenetic and interspecific variability between primate groups (Bromage, 1986; O'Higgins et al., 1991, 2001; Enlow and Hans, 1996; Walters and O'Higgins, 1992). While it is likely that, during growth, some depository fields and, potentially, aspects of condylar, nasal septal, and sutural (Morriss-Kay and Wilkie, 2005) growth are intrinsically regulated, one strong candidate for the extrinsic modulation of remodeling fields is the local mechanical environment (Moss and Salentijn, 1969).

The development of high specification computer systems has paved the way for detailed investigations into the effect of skull loading. Muscle force generation, bony translations, and subsequent stress/strain distributions throughout the skull can all be analyzed using techniques such as finite element analysis (FEA) and multibody dynamics analysis (MDA). These technologies, and in particular the former, have been used for decades in the automotive and aerospace industries to reliably predict structural performance of mechanical systems. Applying FEA and MDA to biological systems seems a logical progression, and indeed mechanical modeling in relation to the masticatory apparatus of humans and other nonhuman primates has previously been conducted (Koolstra and van Eijden, 1995; Daegling and Hylander, 2000; Koolstra, 2003; Sellers and Crompton, 2004; Ross et al., 2005; Strait et al., 2005; Ichim et al., 2006; Kupczik et al., 2007). A common way of estimating loading conditions is to compute physiological cross-sectional areas (PCSA) to approximate the peak forces that can be generated by muscles and, where available to further refine loadings using data from experimental analyses of muscle activation (e.g., Ross et al., 2005). This approach is not applicable in the many circumstances where such data are not available, for example where experimentation and recording of muscle activation or anatomy is not feasible as in fossils. In these circumstances MDA offers an opportunity to estimate muscle forces and facilitates experimentation with muscle architecture and activation patterns. Where experimental data from EMG studies are available, these can be incorporated into MDA models to improve the estimation of loading scenarios.

Most studies load anatomically accurate models and assess the resulting deformations in what is termed an *inductive* approach; however, an alternative *deductive* method is described in work by Witzel and Preuschoft (e.g., Preuschoft and Witzel, 2004; Witzel et al., 2004; Witzel and Preuschoft, 2005). In this *deductive* approach extremely simplified general skull forms are created and then loaded with muscle and bite forces. Compressive stresses drive the "*synthesis*" of the skull, which ends when compressive stresses equilibrate to within set tolerance limits. Both the *inductive* and *deductive* finite element techniques provide important data with respect to skull form and mechanical function, and are described more comprehensively in a recent publication by Rayfield (2007).

To accurately predict the mechanical environment of a skull, not only must the loads (and constraints) be reproduced as faithfully as possible, but the material properties throughout the structure must also be incorporated in the model. However, bone is anisotropic, or at best orthotropic, and its properties vary not only between individuals but also throughout each specimen, therefore defining accurate material properties in a specific skull model is problematic. Strait et al. (2005) conducted a sensitivity study into the effects of using isotropic and anisotropic material properties in a *Macaca fascicularis* cranium and found that even though the more defined models produced greater accuracy in relation to experimental strain results, isotropic material definition produced comparable results. Indeed, a validation study by Kupczik et al. (2007) showed good correlation to experimental data using isotropic material properties, and it is also true that most investigations into complex three-dimensional structures apply isotropic material properties with successful results (e.g., Witzel and Preuschoft, 1999; Rayfield et al., 2001; Cattaneo et al., 2003; Cruz et al., 2003).

The aim of the present study is to investigate the MDA method in predicting the loading conditions of the skull. The main part of the study will describe the novel use of MDA to model skull mechanics of a *Macaca fascicularis*, where muscle forces will drive biting simulations in which bite forces and joint forces will be predicted. We will investigate the role of masticatory muscles in terms of their force application, as well as the importance of geometry and simulating muscle wrapping. In addition to this, the loading derived from the MDA will be applied directly to FEA to assess differences, if any, in the stress distributions between different muscle modeling and loading conditions.

MATERIALS AND METHODS

Micro-computed tomography (CT) skull data from a male crab-eating macaque (*Macaca fascicularis*) were obtained using an X-Tek HMX 160 micro-CT scanner (X-Tek Systems Ltd, Tring, Herts., UK). A 123-kV voltage and 87-μA current were applied in conjunction with a 0.2-mm Cu filter. Voxel resolution was 0.23 mm in the x, y, and z directions. The same CT data were used in a previous study (Kupczik et al., 2007; MAC-14).

MDA

MDA is a technique by which rigid-body motion is defined for an object or group of objects, from which forces can be derived. In relation to the present research, a macaque skull with representative masticatory muscles was modeled. The jaw was subsequently opened to a predefined gape, and in doing so, the muscle groups were extended. From this open position, a simulated food substance was placed between the teeth and then muscle forces were applied to produce biting, where bite and joint reaction forces were recorded.

To produce the MDA model, the micro-CT data were segmented into separate mandibular and cranial portions using AMIRA image segmentation software (Mercury Computer Systems Inc, USA), and three-dimensional surface models were created and exported as wavefront (.obj) files. The surface models were then imported into MSC ADAMS multibody dynamics model-

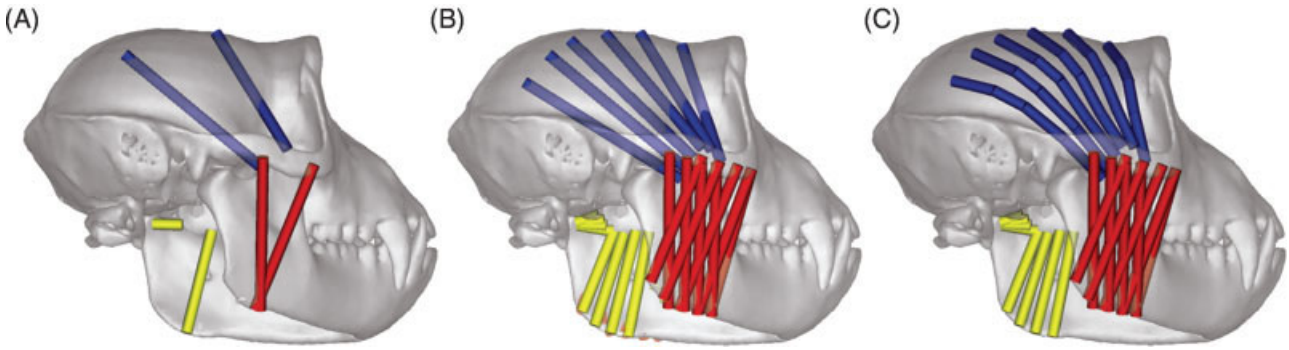

Fig. 1. **A–C:** Multibody dynamics analysis (MDA) models showing single (A), multiple (B), and wrapped (C) muscle groups. Blue, red, and yellow represent the temporalis, masseter, and pterygoid muscle groups, respectively.

ing software (MSC Software Corp, USA), where they were treated as rigid-bodies. Multibody dynamics modeling requires the definition of the mass properties of the moving bodies, the forces or movements applied to them, and the constraints on their movement. The only moving part in this simulation was the mandible, whose mass was calculated from its volume and estimated density. The volume was calculated directly from the AMIRA segmentation software (1.79×10^{-5} m^3), which with an assumed tissue density of 1,050 kg/m^3 (Sellers and Crompton, 2004) gave a mandibular mass of 0.019 kg. The cranium was fixed and the mandible rotated within the temporomandibular joint (TMJ), which was modeled as a bicompartmental joint that could translate in the sagittal plane and rotate about the coronal axis. The skull was initially scanned with the jaw open, which required it to be repositioned into a closed position during the model setup so that the corresponding teeth in the upper and lower teeth rows were aligned. The repositioning from an open to closed state resulted in a posterior translation of 5 mm and an axial rotation of 55°.

The anterior/posterior temporalis, deep/superficial masseter, and medial/lateral pterygoid muscle groups were represented in the model. Initially, the muscle groups were represented by spring elements ("strands"), which were later modified to behave according to realistic force–length characteristics, as defined in equation 1. Three methods of representing the muscle groups were assessed, as shown in Fig. 1: (1) most simply, using single muscle strands for each muscle group directed in a straight line from origin to insertion and positioned centrally within the muscle attachment area; (2) in a more anatomical configuration, using multiple strands for each muscle group directed in a straight line from origin to insertion and applied over the entire muscle area; and (3) as anatomically as possible, using multiple muscle strands for each group combined with muscle wrapping of the anterior and posterior temporalis. For the multiple muscle strand and muscle wrapping models, the anterior and posterior temporalis were split into three sections each, the deep masseter four sections, superficial masseter five sections, and the medial and lateral pterygoids were split into four sections each (see Fig. 1). The three simulations were designed to evaluate the effects of different modeling approaches in providing relevant information to guide future applications. Development of the MDA model to incorporate muscle wrapping of the temporalis muscle groups involved splitting each of the individual muscle strands into four sections, and laying these sections around the cranium. To allow contact between the muscle and the skull contact spheres were placed at the junctions between the muscle sections, as shown in Fig. 2. These contact spheres could slide over the cranium, and for the purposes of the present study, their motion was frictionless.

To open the mandible, the TMJ was moved in such a way that it both rotated and translated (where translation = [5 mm/55°] × gape angle). As the mandible opened the muscle strands elongated and shifted in relation to the underlying structures, except at the points of origin and insertion. The strand force–length characteristics were used to estimate the muscle forces that would generate the opposite motion. Biting simulations were then carried out at a gape of 15° in all muscle models by simulating a stiff, incompressible spring between the teeth and allowing the muscle forces to be applied. A stiff spring (2,000 N/mm stiffness) was positioned bilaterally at the second molar position to represent a rigid food particle. To assess the effect of gape angle and bite point, biting simulations were carried out at 5°, 10°, 15°, 20°, 25°, and 30° at the M2 position, and at 15° gape at the first premolar, first molar, and second molar positions with the multiple muscle strand model.

The muscles were modeled according to Van Ruijven and Weijs (van Ruijven and Weijs, 1990), which were in turn based on a Hill-type model (Hill, 1938):

$$F = F_{max} \times (FA \times FV \times FQ + FP) \quad (1)$$

where F_{max} is maximal tetanic force (25 $N.cm^{-2}$ of cross-section; see for instance Herzog, 1994; Cleuren et al., 1995), FA is a force/length factor, FV is a force/velocity factor, FQ is an activation factor and FP a passive muscle element. The physiological cross-sectional area of the muscles used to calculate F_{max} were taken from the literature (Anton, 1999, 2000; Ross et al., 2005). Equation 1 was simplified to equation 2 because only static biting was simulated (FV = 1 when change in muscle length = 0), FQ was assumed to be 100% (= 1), and FP was excluded for simplicity. The passive element (FP) is attributable to the tendinous structures of the muscle, and contributes to muscle forces beyond a specific gape. The gapes assessed in the present study did not require the representation of the passive element.

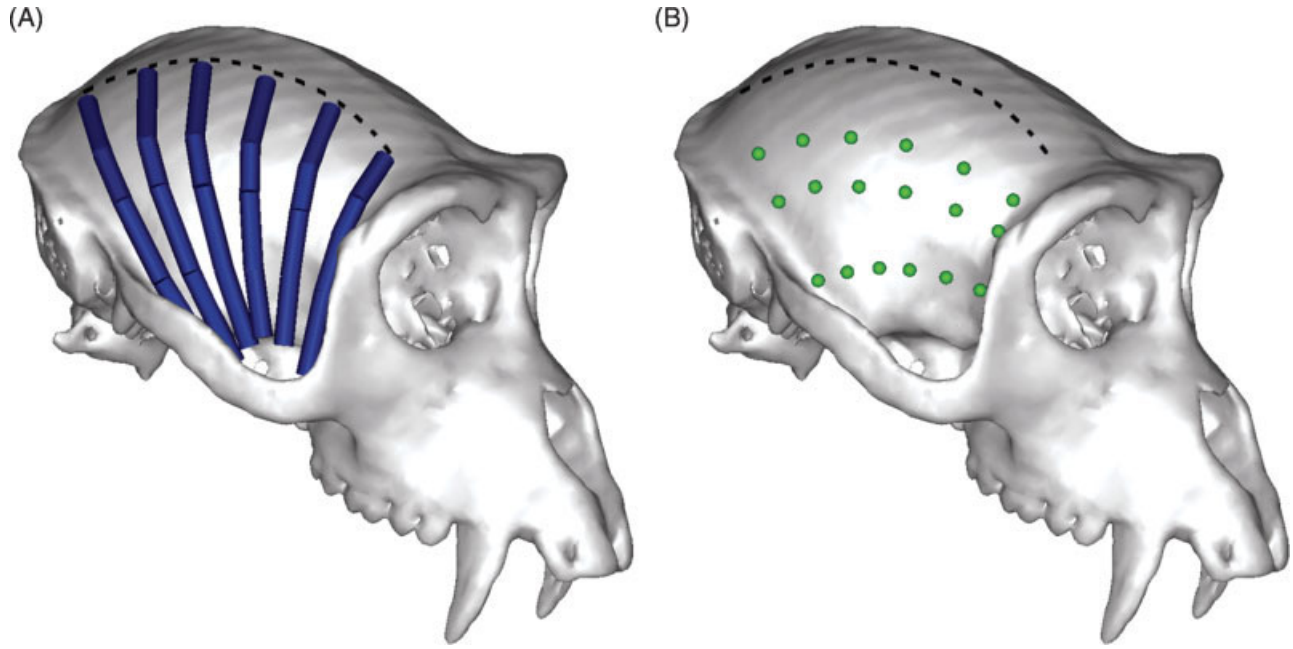

Fig. 2. Temporalis muscle wrapping. **A:** Individual muscle strands are split into four segments and laid around the cranium. **B:** View without the muscle strands showing the contact spheres that connect each of the muscle strand segments. The dotted line represents the attachment point of the muscle on the cranium.

$$F = F_{max} \times FA \quad (2)$$

The force length factor (FA) has been estimated using a second order polynomial, and defines a force–length curve that follows that of experimentally measured skeletal muscle (equation 3; Epstein and Herzog, 1998).

$$FA = -6.25 \times (L/Lo)^2 + 12.5 \times (L/Lo) - 5.25 \quad (3)$$

Where L is the muscle length and Lo is the optimal length, that is, the length at which the muscle can apply its maximum force. For each individual muscle strand, the optimum was specified as its length (Lo) when the model had a gape of 15°. Lo was determined before the biting simulations and was applied as a constant in equation 3. Based on the experience of the authors and what is stated in the literature (Turkawski and van Eijden, 2001), a gape of 15° was deemed reasonable for a macaque. The calculated Lo values are of course approximations, and when more comprehensive data become available this value can be modified.

FEA

In brief, the finite element method works by dividing the geometry of the problem under investigation (e.g., a skull) into a finite number of subregions, called elements, which are connected together at their corners (and sometimes along their mid-sides). These points of connection are called nodes. For stress analysis, a variation in displacement (e.g., linear or quadratic) is then assumed through each element, and equations describing the behavior of each element are derived in terms of the (initially unknown) nodal displacements. These element equations are then combined to give a set of system equations that describe the behavior of the whole problem. After modifying the equations to account for the loading and constraints applied to the problem, these system equations are solved. The output is a list of all the nodal displacements. The element strains can then be calculated from the displacements, and the stresses from the strains. More detailed descriptions of FEA principles and its applications to craniofacial mechanics are available (e.g., Fagan, 1992; Rayfield, 2007; Strait et al., 2007).

ANSYS 11 FEA software (ANSYS Inc, USA) was used in the present study, and like most commercially available FEA software allows stress analyses to be conducted relatively simply. Using AMIRA image segmentation software the cranium surface model (previously created for the MDA analyses) was transformed into a solid model and meshed into approximately 120,000 elements. In ANSYS, isotropic properties were defined with a Young's modulus of 17GPa and Poisson's ratio of 0.3. The Young's modulus and Poisson's ratio values are comparable to those used in other studies (e.g., Strait et al., 2005; Witzel and Preuschoft, 2005); however, the specific values were not critical to the present research, because directly comparable models were being assessed relative to each other and not with anatomical specimens. The loading data were taken directly from the MDA simulations and included bite forces, joint forces, muscle forces, and in the case of muscle wrapping, temporal muscle contact forces. ANSYS then automatically calculated the system equations, incorporated the boundary conditions, performed the solution and calculated the strains and stresses. Because all the loading data was taken directly

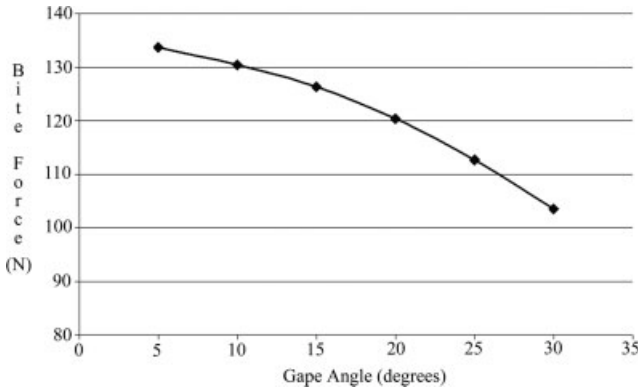

Fig. 3. Effect of gape angle on bite force at the second molar position. Forces are a sum of the right and left sides.

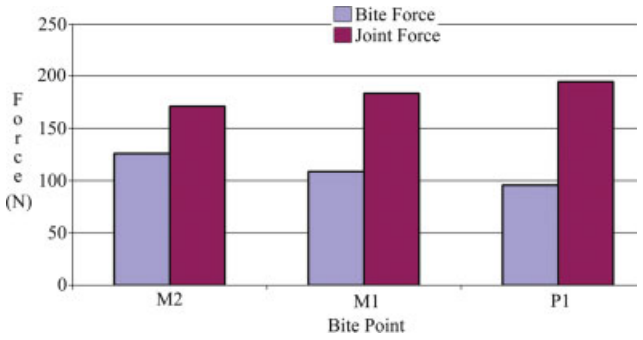

Fig. 4. Effect of bite point on bite force and joint force. Forces are a sum of the right and left sides at a 15° gape. M2, second molar position; M1, first molar position; and P1, first premolar position.

from the MDA simulations, a state of equilibrium was reached, allowing the FE models to be solved with minimal constraints. This resulted in zero reaction forces, with the added benefit of eliminating unrealistically stressed regions at the constraints, which are observed in models that are not in equilibrium.

RESULTS

MDA

All bite force and TMJ force data are a sum of the left and right sides of the skull. At a gape of 15°, bite force and joint force were similar in the single strand, multiple strands and muscle wrapping models (bite force 127.4N ± 0.9N; joint force 170.7N ± 0.6N). Bite force was greatest at lower gapes, reaching a maximum of 133.7N at 5° and a minimum of 103.5N at 30° (see Fig. 3). The second molar biting produced bite forces 30% greater than those at the front of the mouth (126.3N compared with 95.4N), with the greatest joint forces noted at the front of the mouth (Fig. 4). Figure 5 visually displays the contact forces generated by the temporalis muscle groups as they wrapped around the cranium during biting at a 15° gape. A maximum contact force was noted at the anterior portion of the anterior temporalis and reached a value of 6.7N.

Muscle forces vary with gape, because they are a product of the force–length relationships assigned to the muscle strands. Over the range of gapes assessed in the present study, the anterior temporalis showed the maximum variation in muscle force (4N variation from a 15° gape to a 30° gape; single strand model). The multiple muscle strand models showed that force distribution between strands within individual muscle groups also varied with gape. The maximum variation within an individual muscle was noted at a gape of 30° in the anterior temporalis; posterior, middle, and anterior sections of the muscle carried loads of 11.83N, 12.20N, and 12.66N respectively.

FEA

The first principal stress was assessed in the face and vault in the models, as shown in Figs. 6 and 7. The distribution of the stresses was similar in all the models, but the peak values varied. In the face, stresses under the single muscle strand loads were largest (3.33 N/mm^2) in the anterior region of the zygomatic bone (Fig. 6a), with the wrapping multiple strand muscle model with compressive forces producing a value of 2.35 N/mm^2 at the same location (Fig. 6d)—a reduction of 29%. In the vault, application of the temporalis compressive muscle forces reduced the peak stresses in the lower regions significantly (see Fig. 7). For the models with single strand, multiple strand, wrapping, and wrapping with contact forces the peak stress in the lower vault was 0.69N/mm^2, 0.63N/mm^2, 0.49N/mm^2, and 0.11N/mm^2 respectively (peak stress reduction of 84% from a single muscle strand model to a multiple wrapping muscle strand model with compressive forces—see Fig. 7d,b). The inclusion of compressive muscle forces also resulted in a more evenly distributed stress across the entire region.

DISCUSSION

The aim of the present study was to describe the use of MDA in relation to the analysis of a macaque skull. Three methods of representing the jaw adductor muscles were evaluated, namely using single muscle strands, multiple muscle strands, and multiple muscle strands with muscle wrapping. In addition to this, in the muscle wrapping model, muscle contact forces were assessed. Force–length characteristics were assigned to the muscle strands and used to compute the maximum force that each individual muscle can apply with varying gape. Bite force and TMJ force predictions with all three muscle models were similar at a gape of 15° (bite force 127.4N ± 0.9N; joint force 170.7N ± 0.6N), because the total magnitude of muscle forces acting to close the mandible did not vary significantly between the models. This bite force to joint force ratio of 1:1.3 was the same as that reported by Throckmorton and Throckmorton (1985). Dividing the muscles into several strands allowed more detailed analysis of force distributions within different portions of each muscle. As the muscles were extended with increasing gape, the relative extension of the anterior and posterior portions varied; this is potentially important in relation to functioning in vivo and in terms of modeling because the maximum muscle force is related to the length of the muscle fibers. Bite

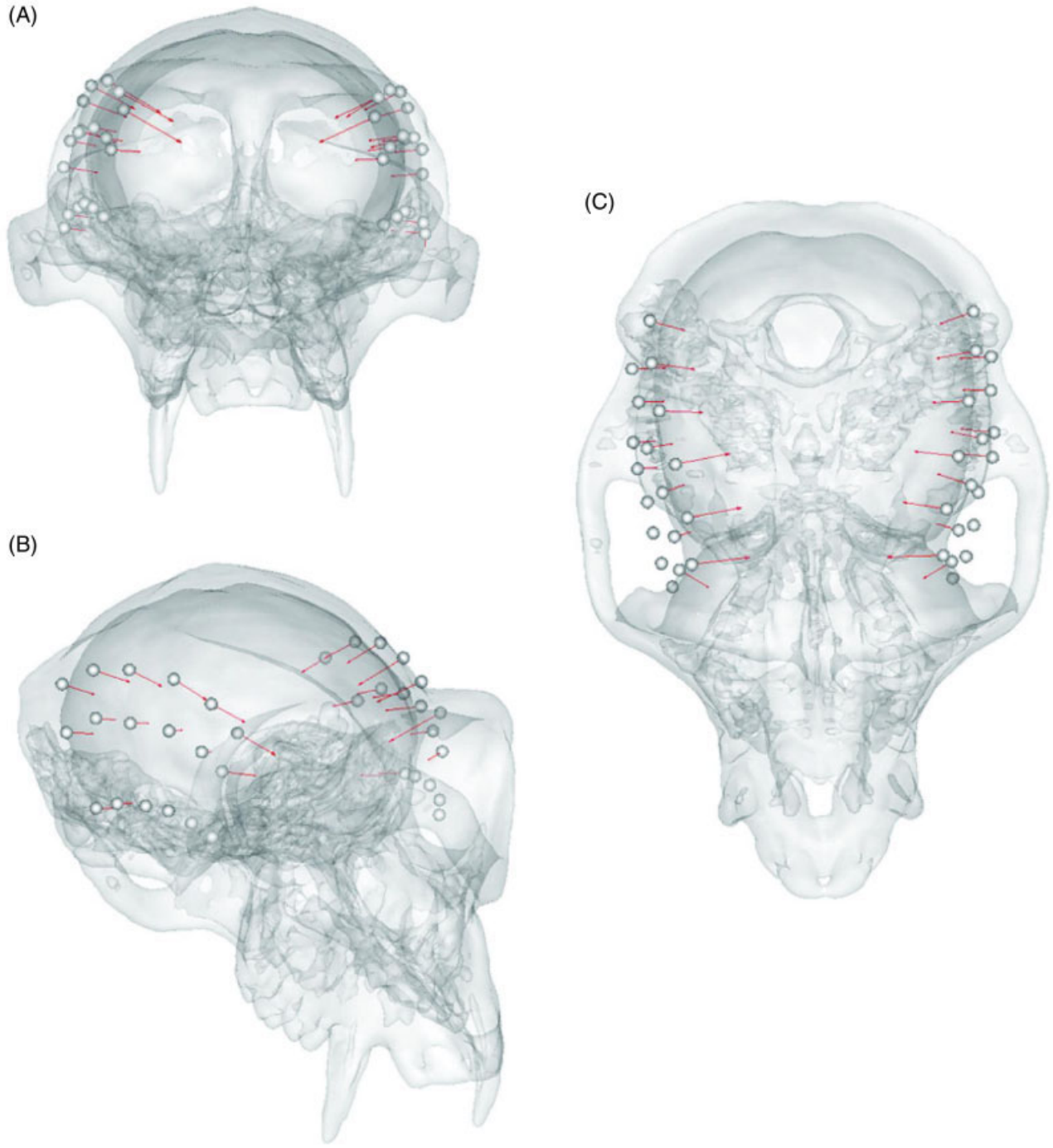

Fig. 5. Visual representation of the contact forces produced during the contraction of the temporalis muscle groups. **A:** Anterior view. **B:** Anterolateral superior view. **C:** Superior view. (The lines show the direction and relative magnitudes of the contact forces).

force reached a maximum at the back of the mouth (second molar position) and reduced steadily as the bite point shifted anteriorly (for the same gape angle). This finding agrees with experimental strain gauge studies (e.g., Pruim et al., 1980; Koolstra et al., 1988). However, others do suggest that in vivo bite forces are lower at the second molar position when compared with the first molar (Mansour and Reynik, 1975; Spencer, 1998). Spencer (1998) observed maximum muscle forces in humans when biting on the first molar, which would be expected to produce the largest bite forces at this position. This finding may, however, be attributable to sen-

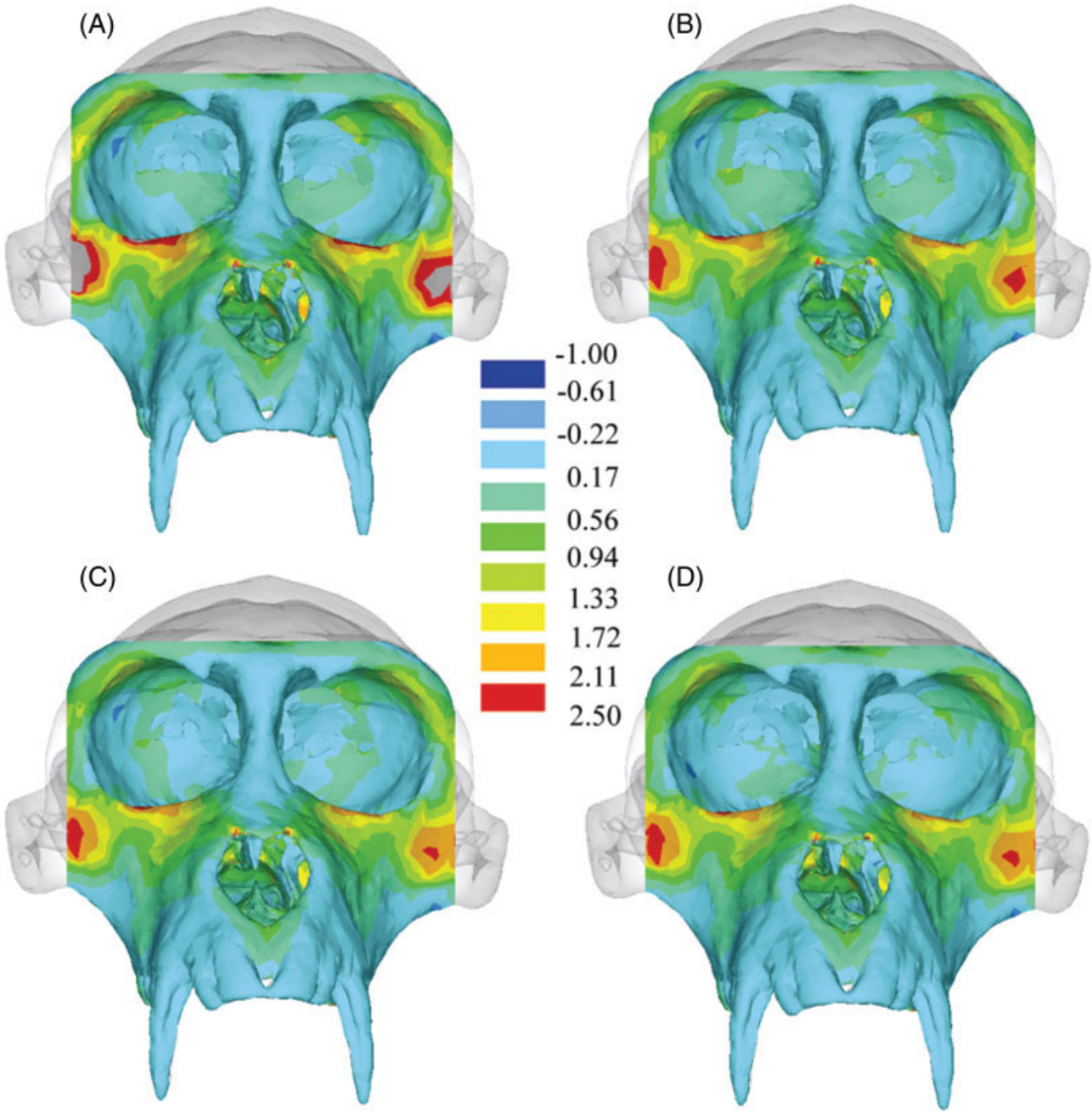

Fig. 6. First principal stress of the face as a result of biting at the M2 position. **A–D:** Represents the results using the single strand load data (A), the multiple strands load data (B), muscle wrapping load data without contact forces (C), and muscle wrapping data with contact forces (D). Units N/mm^2. (The stresses in the gray regions are outside the limits of the contours).

sory rather than biomechanical issues (Koolstra et al., 1988). The predicted TMJ reaction force was highest when biting more anteriorly in the mouth, which agrees with Hylander's findings (1975, 1979). In addition to bite point, gape angle had a notable effect on bite force. There was a significant negative relationship between gape angle and bite force, which agrees with in vivo data obtained by Dumont and Herrel (2003).

Quantitative comparison of the MDA-calculated bite force with those reported in the literature must be undertaken with care, because factors such as applied muscle force, gape angle, and exact food particle position all dictate the bite force produced. It is clear from reported bite force data that these factors along with assumed PCSA values affect the calculated bite forces, with authors reporting values ranging from 678N to 1,080N in humans (Koolstra et al., 1988; Demes and Creel, 1988; Sellers and Crompton, 2004). Assuming the PCSA values of the human masticatory muscles are approximately 5 times larger than those of a macaque

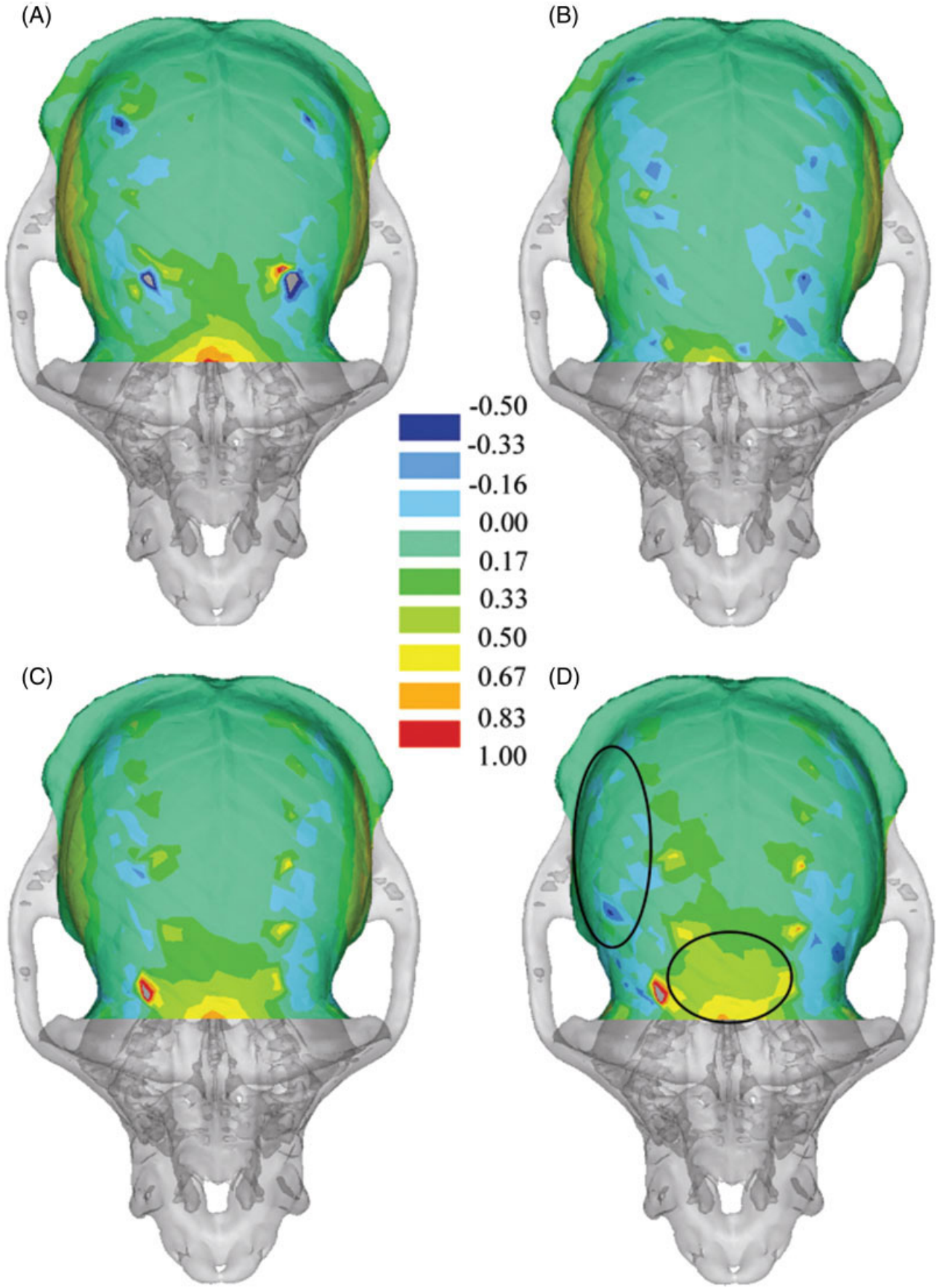

Fig. 7. First principal stress of the vault as a result of biting at the M2 position. **A–D:** Represents the results using the single strand load data (A), the multiple strands load data (B), muscle wrapping load data without contact forces (C), and muscle wrapping data with contact forces (D). Units N/mm^2. (The stresses in the gray regions are outside the limits of the contours). Main areas of interest are circled in d.

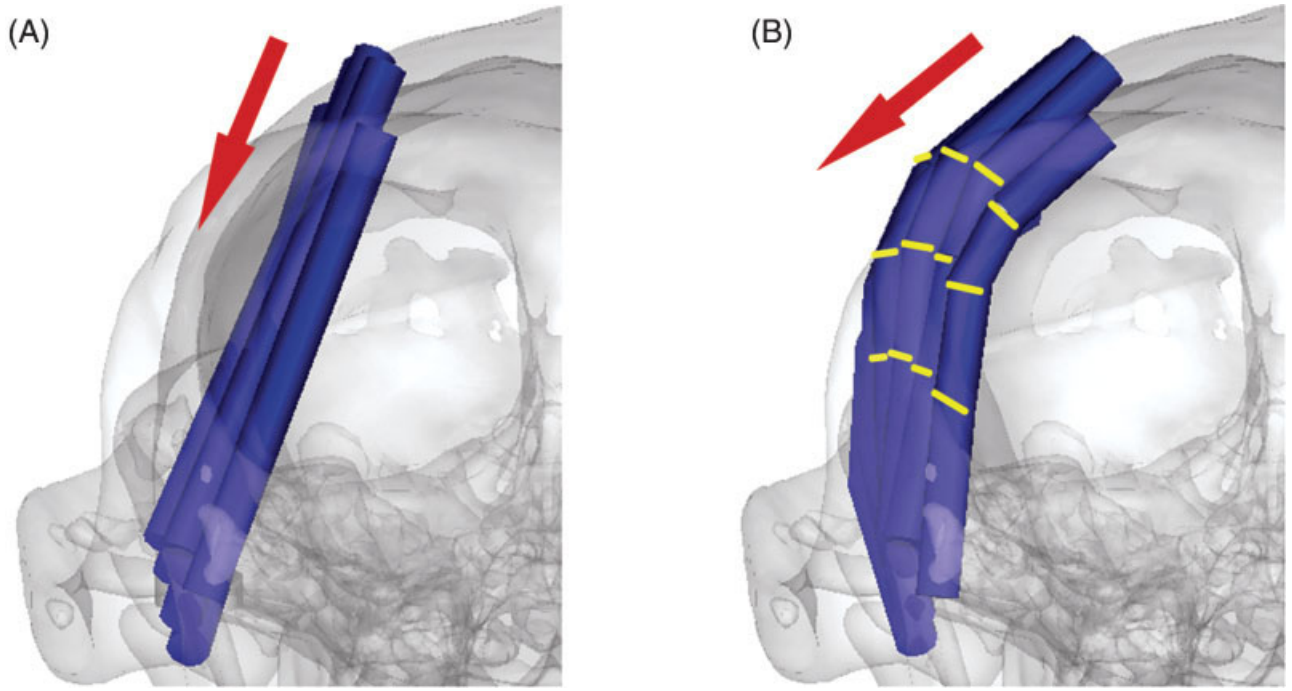

Fig. 8. **A,B:** A sketch showing the direction of the muscle force vector without (A) and with (B) muscle wrapping of the temporalis muscle. The yellow lines highlight the joints between the muscle segments. Anterior view.

(Ross et al., 2005; van Eijden et al., 1997), then by scaling, macaque bite forces might be expected to be 136 N to 216 N. The MDA model in this current study predicted bite forces of 104N to 134N between a gape of 5° and 30° (multiple muscle strand model at the second molar position), and from 95N to 126N between the first premolar and second molar position (multiple muscle strand model at a 15° gape). These results are closer to the values reported by Hylander (1979) who used transducer plates to experimentally record bite forces of between 70N and 120N in macaques.

In FEA of the cranium in which masticatory function is modeled, forces, either in terms of force vectors or force inducting elements, are applied to represent the action of muscles of mastication (e.g., Witzel et al., 2004; Ross et al., 2005; Witzel and Preuschoft, 2005; Strait et al., 2007; Wroe et al., 2007). The application of loading is usually in the form of single force components representing entire muscle groups. More recent studies of skull loading have started to apply forces more widely over muscle attachment regions (e.g., Wroe et al., 2007; Grosse et al., 2007; McHenry et al., 2007). Whether single or several muscle forces are applied, muscle wrapping is rarely included, with only the most recent publications looking into its effects (Grosse et al., 2007). Muscle wrapping has two main consequences when assessing load application; first, the ratio of the orthogonal components of the force vectors vary significantly, as highlighted in Fig. 8. For example, in the anterior-most strand of the anterior temporalis at a gape of 15°, the lateral component of the force vector increased by 135% to 9.4N when muscle wrapping was included. At the same gape, the ventral component reduced by 25% to 9.3N and the posterior component reduced from by 26% to 2.6N. The second important consequence of muscle wrapping is that compressive forces are applied to the skull as the temporalis muscle wraps around the temporal region. Here, we found compressive forces to reach a maximum of 6.7N under the anterior-most portion of the anterior temporalis under biting. The effects of representing muscles as single, multiple, or wrapping strands on stress distributions are shown in Figs. 6 and 7.

Because muscle wrapping was confined to the temporalis muscles the effects on the maxilla and circumorbital regions are limited (Fig. 6). The masseter along with bite forces are the main contributors to stresses in these regions of the face, and the use of a single strand to represent the entire superficial masseter focused all of the force from masseteric contraction on the anterior region of the zygomatic arch, which in turn produced increased stresses in the face (see Fig. 6a). Fanning the muscles over the entire attachment area distributed the masseteric muscle forces along the arch and, as a result, lowered the forces in the face. Ignoring the peak stresses at the muscle attachment points, the vault muscle wrapping tended to put the anterior areas (i.e., the frontal bone) under greater tensile stress, which is attributable to the altered force directions, and in particular the lateral component of the force vector. Including the temporalis contact forces significantly reduced the stresses in the lower vault and resulted in a more uniform stress distribution in this area (Fig. 7d). In future developments of this approach, it will be useful to consider the effect of attaching temporal muscle strands over a wider area, representing the wide attachment area of this

muscle. In the present model, the temporal muscle was only attached to the upper temporal region. If the attachment was distributed over the whole temporal area, its compressive effect in the lower vault may be counteracted, to some extent, by the tensile force produced by the lower muscle strands.

The complexity of skull models is continually increasing, with some models now including a degree of variation in material properties across the skull, muscle groups divided into different segments and the effects of different loading conditions being assessed (e.g., Ross et al., 2005; Strait et al., 2005; Witzel and Preuschoft, 2005; Wroe et al., 2007). MDA offers an opportunity for a further improvement in the biofidelity of these simulations. This study has demonstrated how we can calculate the loading conditions of several muscle groups, joint reaction forces, and bite forces during a single bite simulation, ensuring the skull remains in equilibrium. There are still several assumptions and approximations in the equations used to define the muscles' behavior, which need further development and refinement.

Future application of MDA to model increasingly complex situations should provide novel insights into the optimization of muscle and skull form. For example, *Macaca fascicularis* has a wide and varied diet that includes plants, fruits, seeds, and several small animals (e.g., bird chicks, lizards, frogs). This alone tells us that simulating one loading condition is not enough to fully understand the form of the macaque skull. Variations in bite point, food stiffness, chewing cycles (including possible grinding, shearing, snapping, and so on), as well as forces not arising from mastication such as those arising from expression, head motion, and so on, should also be taken into account in attempting to evaluate craniofacial form in terms of mechanical optimization. In addition, sexual dimorphism clearly plays a pivotal role in shaping the skull, and these differences must lead to differences in skull loading between male and female primates. Beyond obvious variations such as the large canines in the male, other, perhaps less obvious sexually dimorphic variations in muscle attachment zones (e.g., temporalis) and in skeletal form such as the shape of the TMJ bearing surfaces point to differences in loading between the male and female skulls. All these situations can be realized by means of MDA to provide ever more realistic loading data for FEAs.

LITERATURE CITED

Anton SC. 1999. Macaque masseter muscle: internal architecture, fiber length, and cross-sectional area. Int J Prim 20:441–462.

Anton SC. 2000. Macaque pterygoid muscles: internal architecture, fiber length, and cross-sectional area. Int J Prim 21:131–156.

Bromage TG. 1986. A comparative scanning electron microscope study of facial growth remodelling in early hominids. PhD Thesis: University of Toronto.

Cattaneo PM, Dalstra M, Melsen B. 2003. The transfer of occlusal forces through the maxillary molars: a finite-element study. Am J Orthod Dentofacial Orthop 123:367–373.

Cleuren J, Aerts P, De Vree F. 1995. Bite and joint force analysis in caiman crocodilus. Belg J Zool 125:79–94.

Cruz M, Wassall T, Toledo EM, Barra LP, Lemonge AC. 2003. Three-dimensional finite-element stress analysis of a cuneiform-geometry implant. Int J Oral Maxillofac Implants 18:675–684.

Daegling DJ, Hylander WL. 2000. Experimental observation, theoretical models, and biomechanical inference in the study of mandibular form. Am Jf Phys Anth 112:541–551.

Demes B, Creel N. 1988. Bite force, diet and cranial morphology of fossil hominids. J Hum Evol 17:657–670.

Dumont ER, Herrel A. 2003. The effect of gape angle and bite point on bite force in bats. J Exp Biol 206:2117–2123.

Enlow DH, Hans MG. 1996. Essentials of facial growth. Philadelphia: WB Saunders Company.

Epstein M, Herzog W. 1998. Theoretical models of skeletal muscle biological and mathematical considerations. Chichester: John Wiley and Sons. p 23–69.

Fagan MJ. 1992. Finite element analysis: theory and practice. Longmans.

Grosse IR, Dumont ER, Coletta C, Tolleson A. 2007. Techniques for modeling muscle-induced forces on finite element models of skeletal structures. Anat Rec 290:1069–1088.

Herzog W. 1994. Muscle. In: Nigg BM, Herzog W, editors. Biomechanics of the musculoskeletal system. Chichester: John Wiley and Sons. p 154–187.

Hill AV. 1938. The heat of shortening and the dynamic constants of muscle. Proc R Soc B 126:136–195.

Huiskes R. 2000. If bone is the answer, then what is the question? J Anat 197:145–156.

Hylander WL. 1975. The human mandible: lever or link? Am J Phys Anthropol 43:227–242.

Hylander WL. 1979. An experimental analysis of temporomandibular joint reaction force in macaques. Am J Phys Anthropol 51: 433–456.

Ichim I, Swain M, Kieser JA. 2006. Mandibular biomechanics and development of the human chin. J Dent Res 85:638–642.

Koolstra JH. 2003. Number crunching with the human masticatory system. J Dent Res 82:672–676.

Koolstra JH, van Eijden TMGJ. 1995. Biomechanical analysis of jaw-closing movements. J Dent Res 74:1564–1570.

Koolstra JH, van Eijden TMGJ, Weijs WA, Naeije M. 1988. A three-dimensional mathematical model of the human masticatory system predicting maximum possible bite forces. J Biomech 21:563–576.

Kupczik K, Dobson CA, Fagan MJ, Crompton RH, Oxnard CE, O'Higgins P. 2007. Assessing mechanical function of the zygomatic region in macaques: validation and sensitivity testing of finite element models. J Anat 210:41–53.

Mansour RM, Reynik RJ. 1975. In vivo occlusal forces and moments: I. Forces measured in terminal hinge position and associated moments. J Dent Res 54:114–120.

McHenry CR, Wroe S, Clausen PD, Moreno K, Cunningham E. 2007. Super-modeled sabercat, predatory behaviour in Smilodon fatalis revealed by high-resolution 3-D computer simulation. Proc Natl Acad Sci U S A 104:16010–16015.

Morriss-Kay GM, Wilkie AO. 2005. Growth of the normal skull vault and its alteration in craniosynostosis: insights from human genetics and experimental studies. J Anat 207:637–653.

Moss M, Salentijn L. 1969. The primary role of functional matrices in facial growth. Am J Orthop 55:566–577.

O'Higgins P, Johnson DR, Bromage TG, Moore WJ, McPhie P. 1991. A study of craniofacial growth in the sooty Mangabey cercocebus atys. Folia Primatol 56:86–95.

O'Higgins P, Chadfield P, Jones N. 2001. Facial growth and the ontogeny of morphological variation within and between cebus apella and cercocebus torquatus. J Zoo 254:337–357.

Pearson OM, Lieberman DE. 2004. The aging of Wolff's "Law": ontogeny and responses to mechanical loading in cortical bone. Yearb Phys Anthropol 47:63–99.

Preuschoft H, Witzel U. 2004. Functional structure of the skull in hominoidea. Folia Primatol 75:219–252.

Pruim GJ, de Jongh HJ, ten Bosch JJ. 1980. Forces acting on the mandible during bilateral static bite at different bite force levels. J Biomech 13:755–763.

Rayfield EJ. 2007. Finite element analysis and understanding the biomechanics of evolution of living and fossil organisms. Annu Rev Earth Planet Sci 35:541–576.

Rayfield EJ, Norman DB, Horner CC, Horner JR, Smith PM, Thomason JJ, Upchurch P. 2001. Cranial design and function in a large theropod dinosaur. Nature 409:1033–1037.

Ross CF, Patel BA, Slice DE, Strait DS, Dechow PC, Richmond BG, Spencer MA. 2005. Modeling masticatory muscle force in finite element analysis: sensitivity analysis using principal coordinates analysis. Anat Rec A Discov Mol Cell Evol Biol 283:288–299.

Ruff CB, Holt BH, Trinkaus E. 2006. Who's afraid of the big bad Wolff? "Wolff's law" and bone functional adaptation. Am J Phys Anthropol 129:484–498.

Sellers WI, Crompton RH. 2004. Using sensitivity analysis to validate the predictions of a biomechanical model of bite forces. Ann Anat 186:89–95.

Spencer MA. 1998. Force oroduction in the primate masticatory system: electromyographic tests of biomechanical hypothesis. J Hum Evol 34:25–54.

Strait DS, Wang Q, Dechow PC, Ross CF, Richmond BG, Spencer MA, Patel BA. 2005. Modeling elastic properties in finite element analysis: how much precision is needed to produce an accurate model? Anat Rec 283A:275–287.

Strait DS, Richmond BG, Spencer MA, Ross CF, Dechow PC, Wood BA. 2007. Masticatory biomechanics and its relevance to early hominid phylogeny: an examination of palatal thickness using finite-element analysis. J Hum Evol 52:585–599.

Throckmorton GS, Throckmorton LS. 1985. Quantitative calculations of temporomandibular joint reaction forces: I. The importance of the magnitude of the jaw muscle forces. J Biomech 18:445–452.

Turkawaski SJJ, van Eijden TMGJ. 2001. Mechanical properties of single motor units in the rabbit masseter muscle as a function of jaw position. Exp Brain Res 138:153–162.

van Eijden TMGJ, Korfage JAM, Brugman P. 1997. Architecture of the human jaw-closing and jaw-opening muscles. Anat Rec 248: 464–474.

van Ruijven LJ, Weijs WA. 1990. A new model for calculating muscle forces from electromyograms. Eur J Appl Physiol Occup Physiol 61:479–485.

Walters MJ, O'Higgins P. 1992. Factors influencing craniofacial growth: a scanning electron microscope study of high resolution facial replicas. Proc Australas Soc Hum Biol 5:391–403.

Witzel U, Preuschoft H. 1999. The bony roof of the nose in humans and other primates. Zool Anz 238:103–115.

Witzel U, Preuschoft. 2005. Finite element model construction for the virtual synthesis of the skulls in vertebrates: case study of diplodocus. Anat Rec 283A:391–401.

Witzel U, Preuschoft H, Sick H. 2004. The role of the zygomatic arch in the statics of the skull and its adaptive shape. Folia Primatol (Basel) 75:202–218.

Wolff J. 1892. Das Gesetz der Transformation der Knochen (Transl. The law of bone remodelling). Berlin: Springer-Verlag.

Wroe S, Clausen P, McHenry C, Moreno K, Cunningham E. 2007. Computer simulation of feeding behaviour in the thylacine and dingo as a novel test for convergence and niche overlap. Proc R Soc B 274:2819–2828.